Int. J. Electrochem. Sci., 6 **(2011)** 6567 - 6580

International Journal of
ELECTROCHEMICAL
SCIENCE
www.electrochemsci.org

Characterization of the Atmospheric Corrosion of Aluminum in Archipelagic Subtropical Environments

F.J. Hernández[1], *J.J. Santana*[2], *R.M. Souto*[1], *S. González*[1,*], *J. Morales*[1]

[1] Department of Physical Chemistry, Universidad de La Laguna, E-38205 La Laguna (Tenerife, Canary Islands), Spain
[2] Department of Process Engineering, Universidad de Las Palmas de Gran Canaria, Campus Universitario de Tafira, Edificio de Ingenierías, C.P. 35017 Gran Canaria, Spain
[*]E-mail: sjglez@ull.es

Received: 21 September 2011 / *Accepted:* 16 November 2011 / *Published:* 1 December 2011

The atmospheric corrosion of aluminum in archipelagic subtropical environments has been investigated in Tenerife (Canary Islands, Spain). Pitting corrosion has been characterized in terms of the density and depth of the pits. Though longer exposures originate greater pit densities on aluminum, pit size is greatly influenced by the concentration of pollutants and the wetness of the atmospheres. A direct linear relationship between the pitting parameters and the chloride content in the environment was found. The effect of SO_2 is less significant, though electrochemical tests indicate that the addition of sulphate ions to chloride-containing solutions favours the growth of bigger pits.

Keywords: Aluminum; Atmospheric corrosion; Pitting corrosion; Potentiostatic.

1. INTRODUCTION

The spontaneous degradation of metallic materials exposed to the atmosphere is a practical problem with large economic impact in industrialized societies [1]. The influence of the environment can be characterized in terms of its relative humidity, usually expressed in terms of the time of wetness, TOW, (i.e., the total number of hours in a year for which the relative humidity, RH, exceeds 80% while temperature is above 0ºC), and the exposure time, *t*. In addition to these physical variables, the occurrence of chemical species in the atmosphere also affects the extent of atmospheric corrosion, typically those of chloride salts and sulphur or nitrogen oxides, though other pollutants could be eventually encountered. From the combination of weathering factors and concentrations of chemical species, which may also result from anthropogenic activities, atmospheres are then usually classified, as for the characterization of material's degradation, into four main classes, namely rural, urban,

industrial and marine environments [2]. In addition, grades are made within each class to further characterize them with somewhat greater detail. This procedure is widely used to describe atmospheric corrosion worldwide, though its applicability is at least limited in the case of tropical and subtropical regions, and can even be of no use in the case of disrupted territories such as oceanic archipelagos. In the latest case, the wind regimes are strong enough to produce marine environments at locations situated at big distances from the coastline, even at rather high altitudes. A very interesting location for such investigation is offered by the Canary Islands in the Atlantic Ocean, which present a big variety of environments comprised in a rather small geographical region. In this way, characterization of atmospheric corrosion for diverse metals of industrial interest could not be satisfactorily performed in terms of the existing standard procedures based on environmental and meteorological parameters [3-6]. In this way, the standard ISO 9223 norm for the aggressiveness of atmospheres [2], found a very limited applicability, and major discrepancies between predictions and in site measurements were commonly described [5,6]. Discrepancies have also been observed when a much bigger subtropical region such as Cuba Island was investigated [7-10].

To further investigate on this gap in knowledge concerning the degradation of metals occurring in insular subtropical atmospheres, the case of localized corrosion reactions was investigated. They occur in small areas of the exposed surface whereas the rest of the material remains passive. Pitting corrosion is a particular case of localized corrosion in which the corrosive attack occurs in a (very) reduced portion of the surface (often less than 1% of the total exposed surface). In this case, the corrosion reaction progresses in the bulk of the material to greater depths than in the case of generalized corrosion.

The subsequent effect on the corrosion rate is enormous, typically originating values $3x10^4$ to $1x10^6$ times bigger than those experienced by the rest of the surface. Furthermore, current densities comprised between 0.1 and 10 A cm^{-2} are measured inside corroding pits, whereas the surrounding passive surface exhibits values around 10^{-6} A cm^{-2}. To describe the breakdown of the passive layer, and consequently the origin of pitting corrosion, three alternative mechanisms have been proposed in the scientific literature, namely: (1) the *penetration mechanism* [11,12], which involves the transport of anions through the oxide layer towards the underlying metal surface, where they initiate their specific action; (2) the *passive layer breakdown mechanism* [13,14], that requires the local breakdown of the passive layer, thus allowing direct access of the anions to the unprotected metal surface; and (3) the *adsorption mechanism* [15,16], where the process is initiated by the adsorption of the aggressive anions on the oxide layer, thus facilitating the catalytic transfer of metal cations from the oxide layer into the solution.

In every case, aggressive species such as the halide ions (particularly chloride ions due to their abundance in natural media) must be present in the environment. These ions can be easily deformed to penetrate through the lattice of passivating oxides, producing its distortion and forming small interconnecting channels between the metal surface and the aggressive environment. Under such conditions, a (stable) active-passive electrochemical cell is developed, in which the reduction (cathodic) reaction occurs outside the corrosion pit. The high dissolution rates experienced inside the pit cavity arises from the big area ratios occurring between the big cathodic and the small anodic regions.

Aluminum is a metal frequently exposed to the atmosphere in many practical applications, especially in building and aerospace industries among others [17,18]. Various forms of corrosive attack have been found when this metal was exposed to the atmosphere, including pitting corrosion [19-23], intergranular corrosion [21], exfoliation corrosion [17,21], and filiform corrosion [24]. Unfortunately, scarce information is currently available on the characterization of the corrosive behaviour of aluminum in tropical and subtropical regions [4,8]. Furthermore, no attempt has yet been made to correlate field data with the results of accelerated electrochemical tests, which is a severe drawback to quantify the influence of the various environmental parameters in the corrosion mechanism.

In this paper we report the results of an investigation on the atmospheric corrosion of aluminum samples exposed to various locations of Tenerife Island in the Canaries (Spain) which correspond to different subtropical environments.

The work was complemented with accelerated laboratory tests using electrochemical techniques to analyze the effect of the atmospheric pollutants on this process.

2. EXPERIMENTAL.

Six corrosion stations were set up in the locations marked in Figure 1.

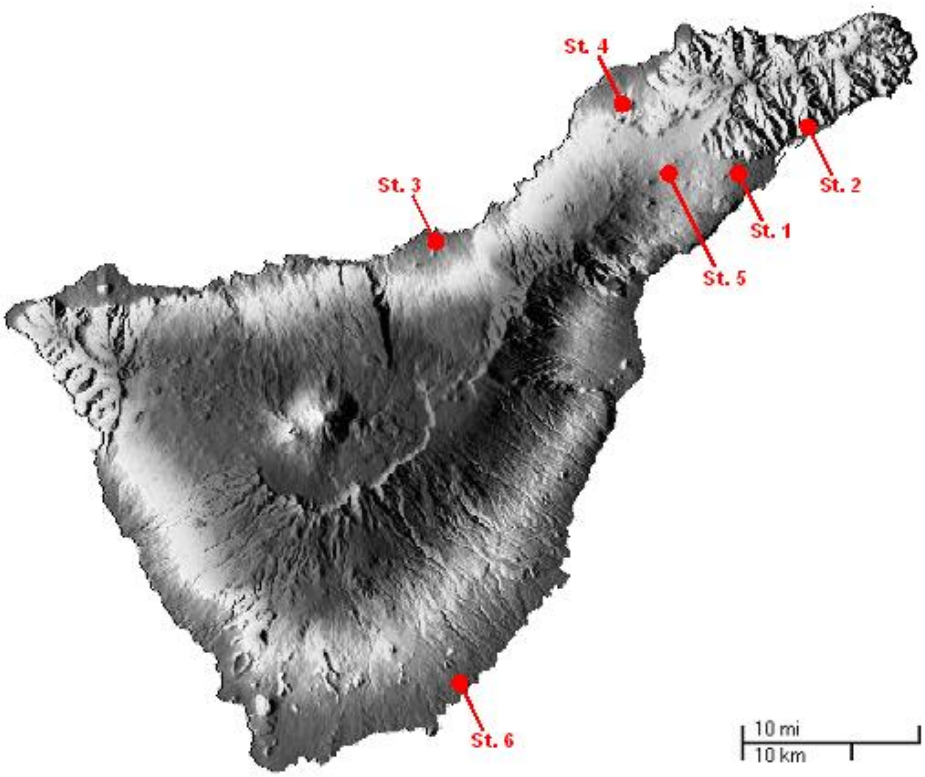

Figure 1. Geographical distribution of corrosion test sites on the island of Tenerife.

These stations cover the typical range of environmental conditions (urban, rural, marine and industrial) as encountered in the Tenerife Island.

Table 1. Geographic coordinates and type of atmospheres of the test sites.

Exposure Station		Geographic coordinate		Elevation (m)	Distance from coast line (m)	Atmosphere
No.	Location	North Latitude	West longitude			
1	Instituto Meteorológico de las Canarias Occidentales	28º27'18''	16º14'56''	36	1100	Urban
2	Instituto Oceanográfico de Canarias	28º30'03''	16º11'49''	2	50	Marine
3	Jardín Botánico	28º24'06''	16º31'30''	120	1100	Rural
4	Finca "La Garimba"	28º29'52''	16º23'05''	500	3000	Rural
5	Facultad de Química	28º28'10''	16º19'04''	600	6200	Urban
6	Central de UNELCO	28º02'34''	16º34'14''	12	200	Industrial

Table 1 lists the main characteristics of these locations. The stations consisted in a painted metallic structure, which supported the metal test pieces fixed to the structure using nylon screws in order to avoid galvanic coupling processes. The traps employed to capture the pollutants present in air were fixed to the rear of the station's metallic structure. SO_2 determinations were made using the Husy method [25], whereas chlorides were detected using the damp toggle method described in the 9225:1992 (E) ISO norm [26]. These pollutants were analyzed every two weeks over a 6-months period. The metal test pieces were 100 mm x 40 mm x 2 mm in size, and they were duly tagged for precise identification. The metal plates are aluminum 99.5% purity, and they contain minor amounts of Si, Fe, Mn, Zn and Ti as given in Table 2. This composition satisfies the UNE L-3051 norm [27]. In order to determine the corrosion rate, the test pieces were cleaned as described in the G1-90ASTM norm [28]. Test coupons were picked from site every two weeks for their analysis.

Table 2. Chemical composition of aluminum plates.

Element	Base Al	Si	Fe	Mn	Zn	Ti	Other
Content (%)	Balance	0.30	0.40	0.05	0.10	0.05	0.03

Electrochemical studies were performed using 99.5% purity aluminum plates cut to 20 mm x 40 mm x 2 mm. Prior treatment of the samples involved a sequence of steps, namely thorough washing with distilled water and soap, rinsing in distilled water, grinding with 800 and 1000 grit emery paper, and polishing with 0.3 μm size alumina powder until mirror appearance. They were washed in acetone inside a ultrasound bath, further rinsed with distilled water, and dried in a glass container under vacuum. To remove any mechanical stresses arising from the material, a thermal treatment involving the heating of the samples for 4 hours in the 180-210 ºC range, a temperature lower than that required

for the recrystallization of the metal, thus avoiding changes in the microstructure to occur. Both heating and cooling steps were performed at a very low rate to avoid the development of further stresses in the samples.

The aluminum samples were placed in a Thai's electrochemical cell using a three-electrode configuration. A saturated calomel reference electrode and a platinum auxiliary electrode completed the cell. The system was purged under argon atmosphere for 3 hours until a stable open circuit (OCP) measurement was attained. Potentiodynamic polarization measurements were performed starting from -250 mV from OCP until +1500 mV from OCP, and subsequently the potential direction was reversed back to the starting potential. The scan rate was 0.5 mV s^{-1}. The test electrolyte employed was 0.05 M NaCl + x M Na_2SO_4, with the following values of x: 0, 10^{-3}, 10^{-2} and 10^{-1}.

3. RESULTS AND DISCUSSION

3.1. Atmospheric exposure

Tenerife is the largest island of the Canarian Archipelago. It has a surface area of 2,034 square kilometres and is in a central position between the islands of Gran Canaria, La Gomera and La Palma. The shape of the island looks like an irregular triangle (see Figure 1), and at its centre, it rises Mount Teide, the highest mountain at 3,718 metres above sea-level. Tenerife is characterized by an atmospheric regime characteristic of subtropical latitudes, the proximity to a continent, surrounded by the cold Canary Stream, in addition to its abrupt orography. These conditions originate a gentle climate, wetter and cooler in the north, whereas more arid in the south. Contrary to other marine areas, thermal inversion with altitude results in lower relative humidities at places close to the sea shore compared to those at altitudes above 600 meters high, because the Trade Winds influence the climate up to 1500 meters high. These observations are reflected in the TOW values shown in Figure 2, with higher TOW values being observed at the stations located in the northern side of the island (stations 3, 4 and 5).

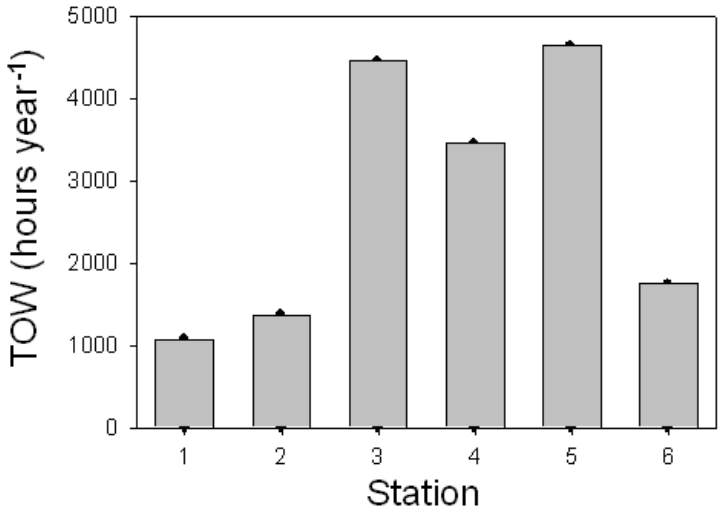

Figure 2. TOW values registered in the six test stations.

The distributions of pollutants that can be found in a variety of atmospheres present in the island of Tenerife, covering urban, industrial, rural and marine locations, can be observed from the inspection of Figure 3.

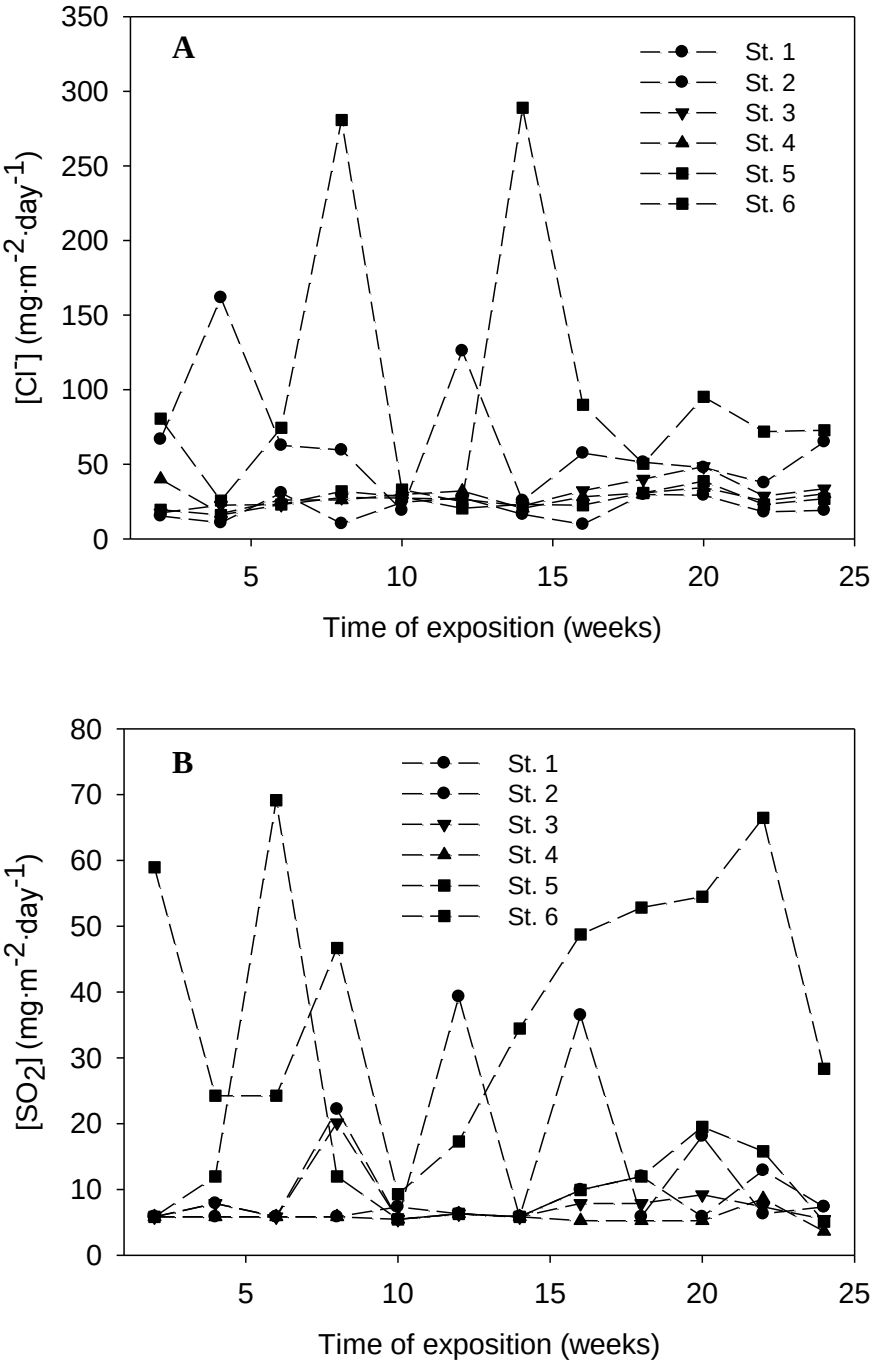

Figure 3. Chloride and sulphur dioxide deposition rate for six-month exposures.

Plots of the variations of chloride and SO_2 contents (expressed as mg m^{-2} day^{-1}), monitored over the duration of the exposures, are depicted in parts a) and b) of Figure 3, respectively. In all the cases, high chloride contents corresponding to marine atmospheres are observed, though some

locations are situated several kilometers from the seashore, and even one of them was placed at an altitude of 610 meters above the sea level (cf. Table 1). Conversely, rather low SO_2 contents were found, even for those locations established in urban and industrial areas. The latest is very significant because a refinery was the main industry in the area. These observations concerning pollutants in the air can be explained by considering that in a highly fragmented territory such an archipelagic island in a subtropical geographical location, the predominant direction of marine winds greatly conditions the distribution and contents of the atmospheres to be found. Accordingly, chloride ions become the main aggressive species in the atmosphere towards the degradation of materials. On the other hand, the TOW values are also very high in all the cases, again due to the high humidity of the winds blowing inland from the ocean during most of the year [6]. The aggressive effect of pollutants on a metallic material is constrained to the development of a humid layer over the metal surface. Thus, for a given pollutant content, longer times of wetness result in greater corrosive effects.

The corrosive attack of aluminum samples exposed in the corrosion test sites is initiated with the development of humid layers on the surface of the samples, which contain the pollutants present in the atmosphere, and originate pits on the metal surface. Figure 4 shows SEM micrographs of the corroded surfaces in which the formation of pits and corrosion products can be observed. The pitting corrosion processes are promoted by the chloride ions contained in the marine aerosols [29], because sodium ions favor higher pH values in the cathodic sites, which originate the alkaline dissolution of the passivating film of alumina [20]. With the elapse of time, and due to the blockage of the anodic sites inside the corrosion pits by precipitated corrosion products, the dissolution reaction of aluminum initiates from the pit borders. Therefore, the corrosive attack progresses in the surface of the metal originating a distribution of swallow pits of irregular shapes. Though the characterization of the corrosion products was not attempted in this study, the formation of precipitates with dendritic shapes can be reported from the observation of the SEM micrograph given in Figure 4B, a feature commonly found in aluminum and its alloys [30].

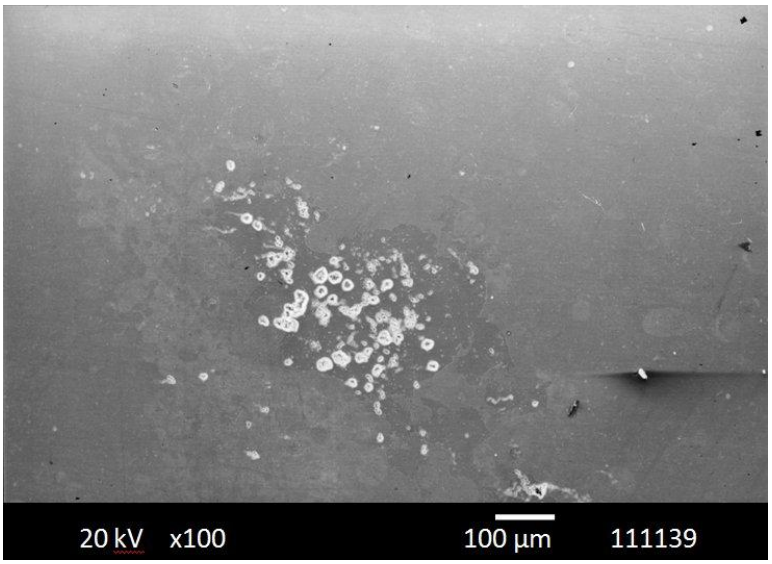

A

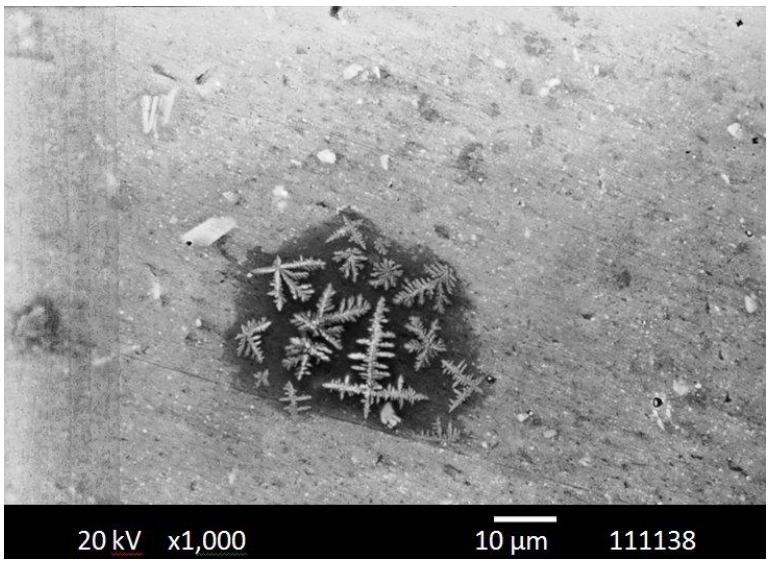

B

Figure 4. SEM micrographs of pit nucleation (A), and the formation of corrosion products inside pits (B), during the atmospheric corrosion of aluminum.

Figures 5 and 6 illustrate the changes in pit density and pit depth with exposure in the different test sites. These two parameters were determined from the same areas in the samples by means of a metallographic microscope that could be focused on either the bottom of the pits and the surface of the sample. The values are the average of measurements performed from the deepest 10 pits. It can be concluded that both the depth and the density of the pits increase with longer exposures. A direct relationship between the number of pits and the elapse of time could not be established from these data, which may be taken as an indication for the random nature of the pitting process, both in terms of space and time.

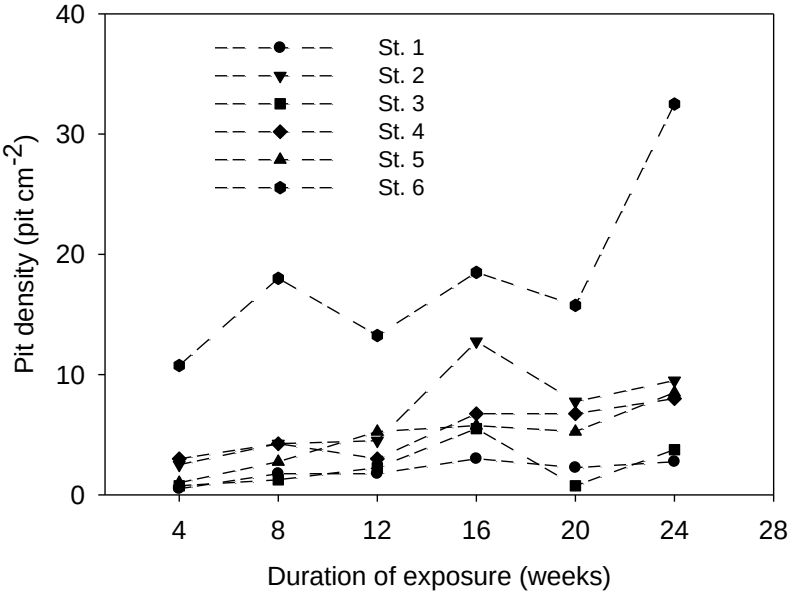

Figure 5. Time course of pit density values from samples exposed in the various test sites.

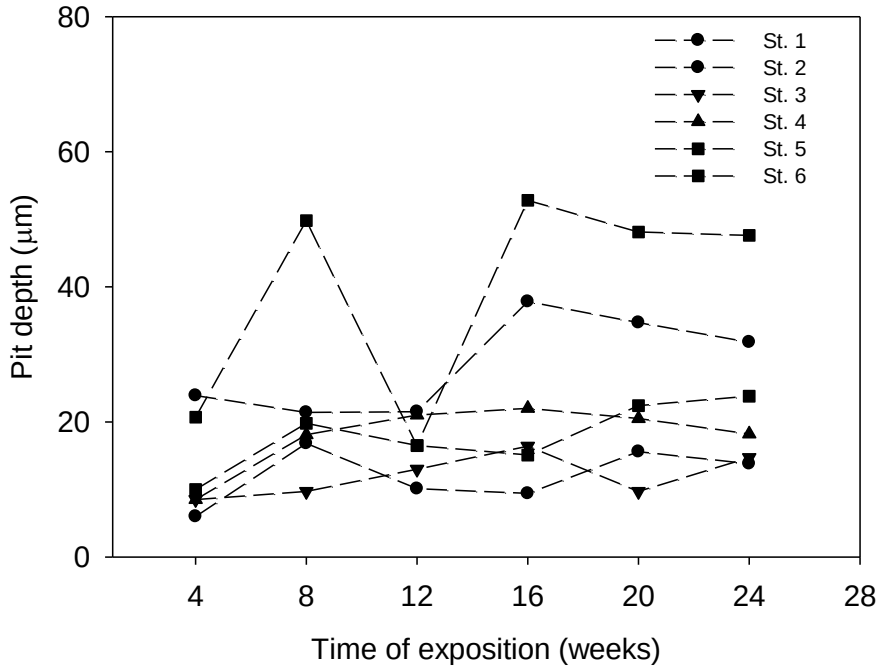

Figure 6. Time course of the mean pit depth values from samples exposed in the various test sites.

The dependences of pit depth and density as a function of chloride and SO_2 contents, and TOW are plotted in Figure 7.

A linear relationship between the pit parameters and the chloride concentration is found for the test sites under investigation, and the correlation factors amounted 0.90 and 0.97 for the density and the depth, respectively (cf. Figure 7A). Linear relationships between these pitting parameters and the concentration of SO_2 can also be determined, though correlation factors are less satisfactory this time, namely 0.90 with the pit density, and 0.70 with the pit depth. A closer inspection of the Figure 7B leads to the observation that most of the data occur in the left bottom corner of the graph, and that they present a major scatter. Thus, from these data no significant influence of SO_2 component towards the onset of pitting corrosion in aluminum in these locations can be concluded. This observation may be related to the low adsorption of this pollutant on aluminum [30], and its minor effect towards aluminum corrosion occurring in highly humid environments [1]. On the other hand, TOW values depicted in Figure 7C indicate that lower pitting occurs in the stations located in the wetter north side of the island (i.e., stations 3, 4 and 5), though greater values are found with the increase of TOW in this case. Conversely, the greater values of the pitting parameters are found from stations 2 and 6, which are closer to the sea and thus under the influence of marine aerosols. Therefore, chloride contents seem to exert the greatest corroding effect, whereas time of wetness produces a smaller, yet significant, influence too.

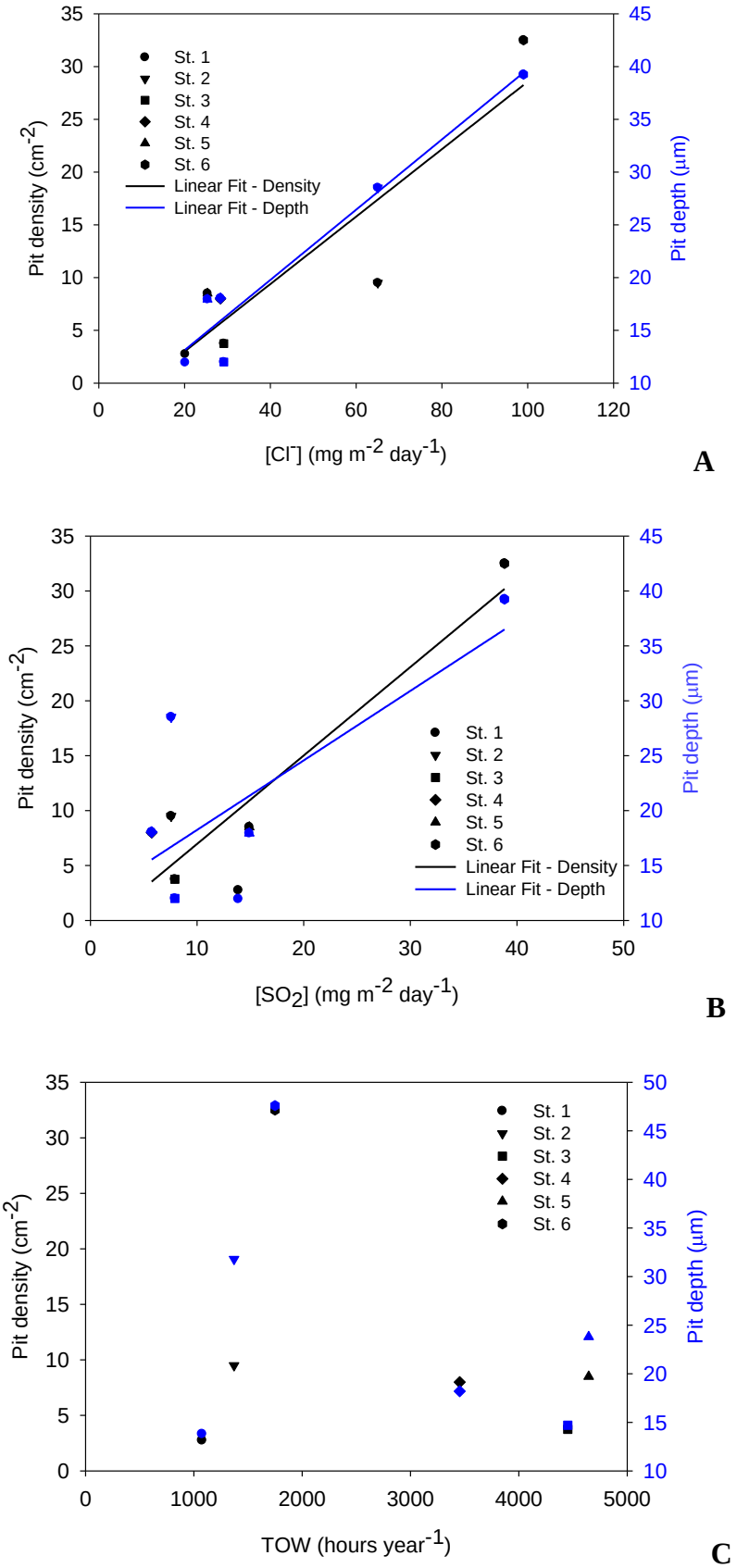

Figure 7. Representations of the pit density and mean pit depth as a function of (A) chloride content, (B) SO_2 content, and (C) TOW from samples exposed in the various test sites.

3.2. Electrochemical tests

Laboratory tests were also performed with the objective to ascertain the influence of pollutant's concentration on the evolution of pitting in aluminum.

Cyclic polarization curves were recorded, at v = 0.5 mV s^{-1} between -0.25 and +1.50 mV from OCP, for metal plates immersed in NaCl + Na_2SO_4 aqueous solutions of various concentrations. Figure 8 shows a typical polarization curve obtained for a plate immersed in 0.05 M NaCl + 0.1 M Na_2SO_4 solution. Instabilities related to metastable formation of pits are observed shortly after the positive-going potential scan passed the OCP value, whereas the breakdown potential is the potential where current increases abruptly with increasing potential (i.e., at about -0.20 V vs. SCE in this case). After the complete cyclic polarization curve was acquired, the pits formed during the potential excursion were characterized by using SEM in a similar manner to that previously employed with the samples from atmospheric exposures.

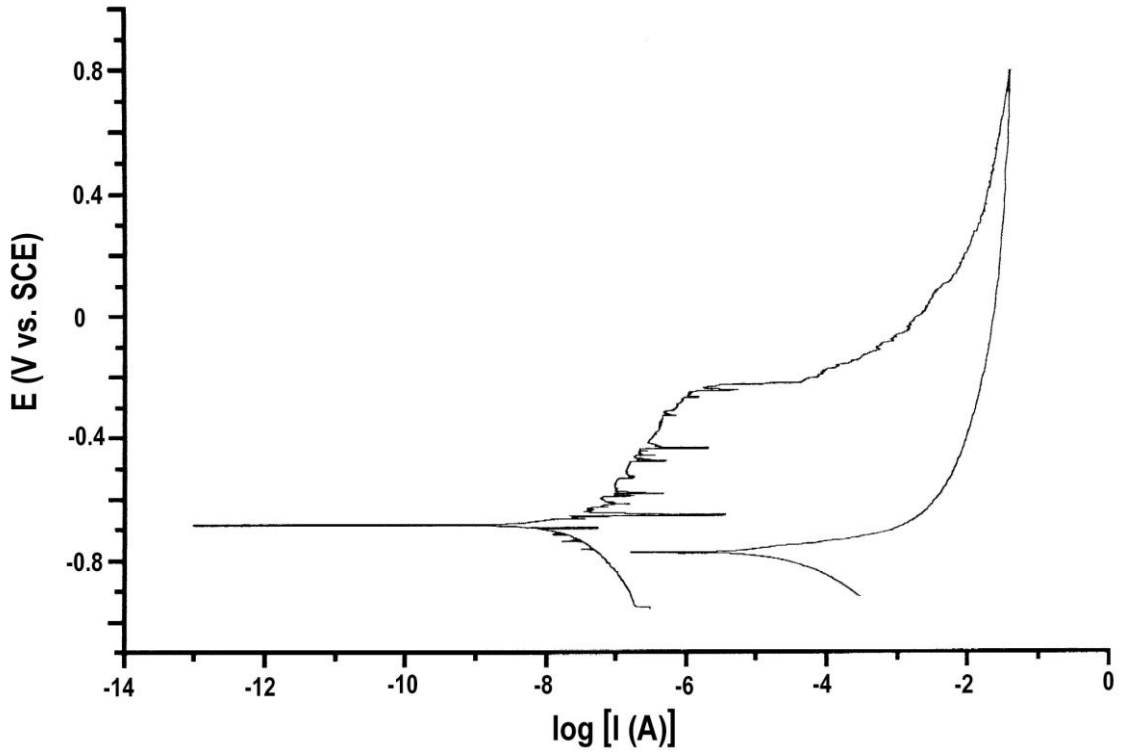

Figure 8. Cyclic polarization curve of an aluminium plate immersed in 0.05 M NaCl + 0.1 M Na_2SO_4 solution. Scan rate: 0.5 mV s^{-1}.

Figure 9 gives the changes in density, depth and diameter of the pits observed when one or both pollutants were present in the electrolytic phase, as well as with changes in their concentrations. Pit density is observed to decrease with the increase of sulphate concentration, due to the competitive adsorption of chloride and sulphate anions on the metal. This competitive adsorption effect may also be responsible for the fact that greater pit depths are found with the increase of sulphate concentration. Chloride and other halide ions may eventually inhibit the active dissolution of metals by replacing OH^-

ions from the interphase, and the partial replacement of chloride by sulphate may contribute to enhanced dissolution inside the pits.

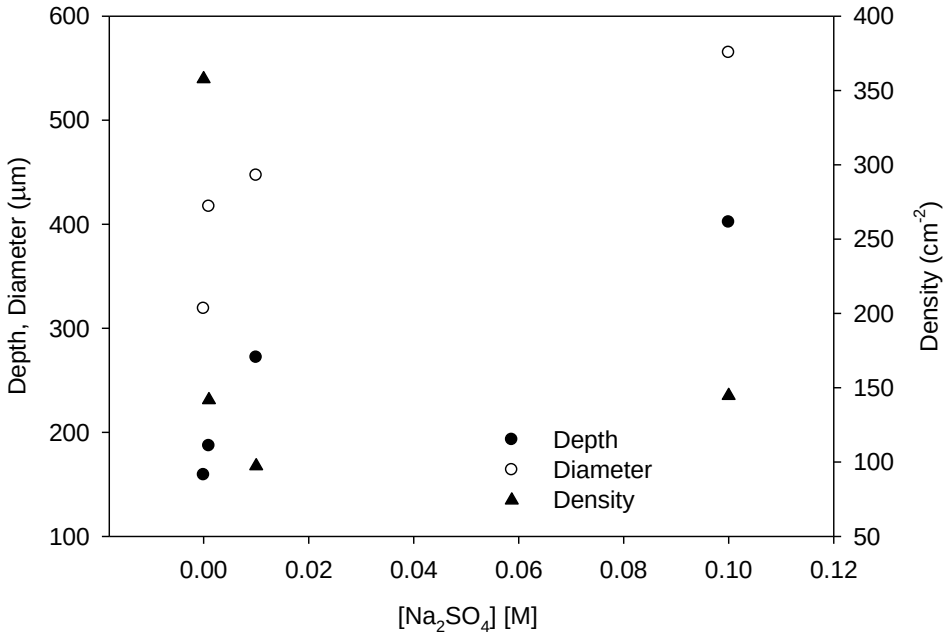

Figure 9. Representations of the pit density, average pit diameter and average pit depth determined aluminum samples after completing the potentiodynamic polarization experiments in 0.05 M NaCl + *x* M Na_2SO_4.

SEM micrographs depicted in Figure 10 also assist the characterization of the advancement of pitting corrosion in these electrolytes. When chloride ions are the only pollutants present in the aqueous solution (cf. Figure 10A), the corrosive attack results in the formation of a rather big number of corrosion pits. The addition of sulphate ions to the environment brings about a reduction in the number of pits nucleated on the metal surface, though they exhibit bigger depths and diameters (see Figures 10B and 10C). This trend changes for the sample tested in the electrolyte with the highest sulphate concentration shown (i.e., 10^{-1} M, Figure 10D).

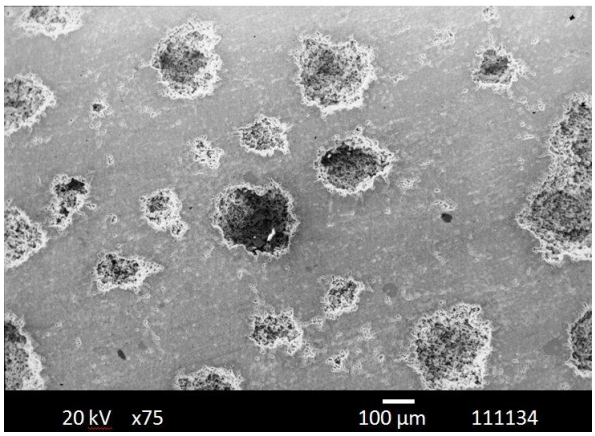

A

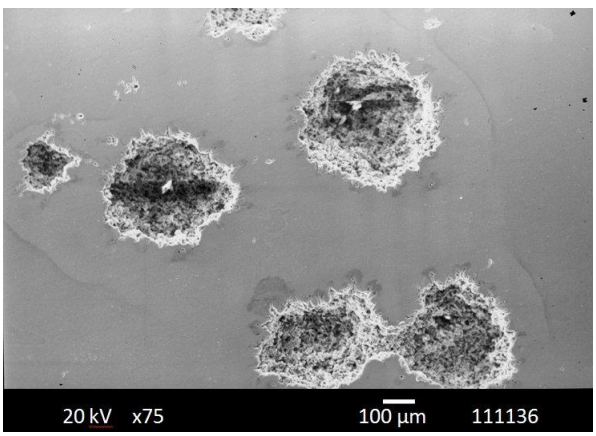

B

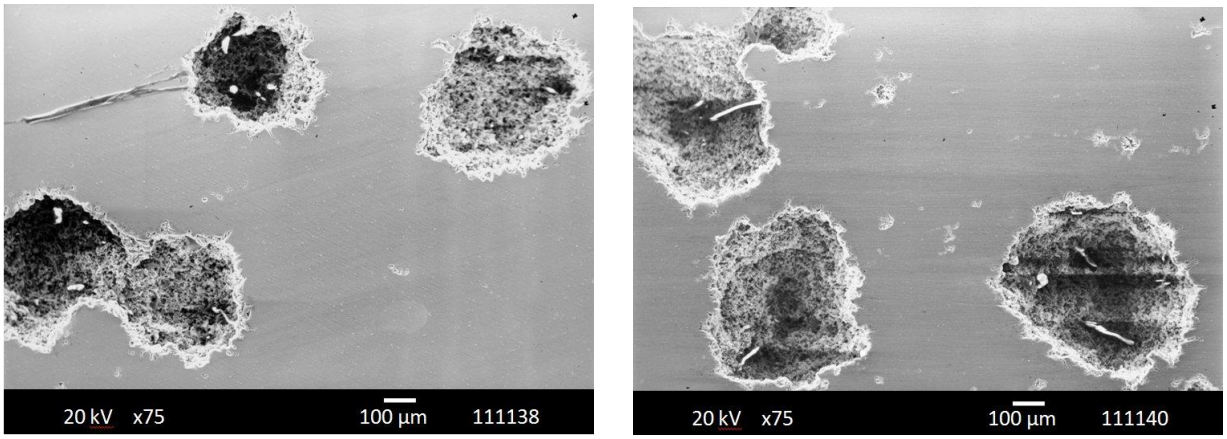

C **D**

Figure 10. SEM micrographs taken after completing the potentiodynamic polarization experiments described in the text on alumimium plates immersed in solutions of composition: A) 0.05 M NaCl; B) 0.05 M NaCl + 10^{-3} M Na_2SO_4; C) 0.05 M NaCl + 10^{-2} M Na_2SO_4; and D) 0.05 M NaCl + 10^{-1} M Na_2SO_4.

4. CONCLUSIONS

(1) In general, longer exposures of aluminum samples to atmospheres in the island of Tenerife result in higher pit densities as well as the pits growing deeper from the surface, though the magnitude of the latter effect greatly depends on the composition of the local environments.

(2) Linear relationships on pollutant concentrations, namely chloride ions and SO_2, could be established for both the pit densities and the pit depths.

(3) Competitive adsorption of chloride and sulphate ions on the metal surface occurs when these species are simultaneously present in the aqueous phase. The number of pits induced in an electrochemical cell decrease with the increase of sulphate concentration in the electrolyte, though the average pits grow to greater diameters and depths in the presence of sulphate ions.

ACKNOWLEDGEMENTS
This work was supported by the Ministerio de Ciencia y Tecnología (Madrid, Spain) and the European Regional Development Fund (Brussels, Belgium) under Project No. CTQ2009-14322, and by University of La Laguna (Proyecto de carácter estructurante en Cambio Climático). A grant awarded to JJS by the Gobierno de Canarias (Spain) to conduct a research stay at the University of La Laguna is gratefully acknowledged.

References

1. I.L. Rozenfeld, *Atmospheric corrosion of Metals*, National Association of Corrosion Engineers, Houston (1972).

2. ISO 9223, *Corrosion of Metals and Alloys-Classification of Corrosivity of Atmospheres*, ISO, Geneva (1990).
3. J .J. Santana Rodríguez, F. J. Santana Hernández, J. E. González González, *Corros. Sci.*, 44 (2002) 2597.
4. J. J. Santana Rodríguez, F. J. Santana Hernández, J. E. González González, *Corros. Sci.*, 45 (2003) 799.
5. J. Morales, S. Martín-Krijer, F. Díaz, J. Hernández-Borges, S. González, *Corros. Sci*., 47 (2005) 2005.
6. J. Morales, F. Díaz, J. Hernández-Borges, S. González, V. Cano, *Corros. Sci*., 49 (2007) 526.
7. A.R. Mendoza, F. Corvo, *Corros. Sci.*, 42 (2000) 1123.
8. F. Corvo, J. Minota, J. Delgado, C. Arroyave, *Corros. Sci*., 47 (2005) 883.
9. F. Corvo, T. Pérez, Y. Martin, J. Reyes, L. R. Dzib, J. A. González, A. Castañeda, *Corros. Sci.*, 50 (2008) 206.
10. F. Corvo, T. Perez, L. R. Dzib, Y. Martin, A. Castañeda, E. Gonzalez, J. Perez, *Corros. Sci*., 50 (2008) 220.
11. C.Y. Chao, L.F. Lin, D.D. MacDonald, *J. Electrochem. Soc*., 128 (1981) 1187.
12. C.Y. Chao, L.F. Lin, D.D. MacDonald, *J. Electrochem. Soc.*, 128 (1981) 1194.
13. N. Sato, *Electrochim. Acta*, 16 (1971) 1683.
14. N. Sato, K. Kudo, T. Noda, *Electrochim. Acta*, 16 (1971) 1909.
15. Y.M. Kolotyrkin, *J. Electrochem. Soc*., 108 (1961) 209.
16. H. P. Leckie, H. H. Uhlig, *J. Electrochem. Soc*., 113 (1966) 1262-1267.
17. R. T. Foley, *Corrosion*, 42 (1986) 277.
18. R. Z. Nakazato, E. N. Codaro, L. M. F. Ribeiro, L. R. O. Hein, *Prakt. Metallogr*., 38 (2001) 301.
19. A.S. Elola, T. F. Otero, A. Porro, *Corrosion*, 48 (1992) 854.
20. D. Bengtsson Blücher, J.-E. Svensson, L.- G. Johansson, *Corros. Sci.*, 48 (2006) 1848.
21. R. Vera, D. Delgado, B. M. Rosales, *Corros. Sci*., 48 (2006) 2882.
22. M. Natesan, G. Venkatachari, N. Palaniswamy, *Corros. Sci*., 48 (2006) 3584.
23. D. de la Fuente, E. Otero-Huerta, M. Morcillo, *Corros. Sci*., 49 (2007) 3134.
24. J. A. González, M. Morcillo, E. Escudero, V. López, E. Otero, *Surf. Coat. Technol*., 153 (2002) 225.
25. ISO/TC 156 N 250. *Corrosion of Metals and Alloys. Aggressivity of Atmospheres. Methods of Measurements of Pollution Data*, ISO, Geneva (1986).
26. ISO 9225:1992(E); *Corrosion of Metals and Alloys – Corrosivity of Atmospheres –Measurement of Pollution*, ISO, Geneva (1992).
27. UNE 38114:2000 Norm, *Aluminio y Aleaciones de Aluminio para Forja*, AENOR, Madrid (2000).
28. ASTM G1-90, *Standard Practice for Preparing, Cleaning and Evaluating Corrosion Test Specimens*, 1990.
29. J. H. Seinfeld, S. N. Pandis, *Atmospheric Chemistry and Physics: From Air Pollution to Climate Change*, John Wiley & Sons, New York (1998).
30. S. Henry, T. Minghetti, M. Rappaz, *Acta Mater.*, 46 (1998) 6431.
31. T. Sydberger, N.- G. Vannerberg, *Corros. Sci.*, 12 (1972) 775.